

Enlarging the π System of Phosphorescent ($C^{\wedge}C^*$) Cyclometalated Platinum(II) NHC Complexes

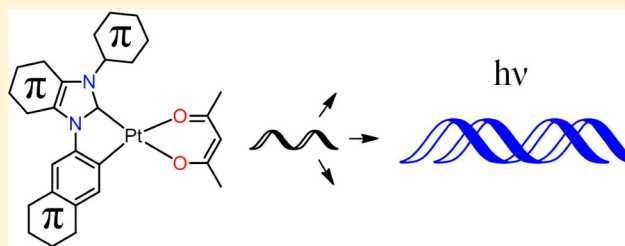
Alexander Tronnier,[†] Alexander Pöthig,^{†,§} Stefan Metz,[‡] Gerhard Wagenblast,[‡] Ingo Münster,[‡] and Thomas Strassner^{*,†}

[†]Physikalische Organische Chemie, Technische Universität Dresden, 01069 Dresden, Germany

[‡]BASF SE, 67056 Ludwigshafen, Germany

S Supporting Information

ABSTRACT: Cyclometalated ($C^{\wedge}C^*$) platinum(II) *N*-heterocyclic carbene (NHC) complexes are emerging as a new class of phosphorescent emitters for the application in organic light-emitting devices (OLEDs). We present the synthesis of six new complexes of this class to investigate the influence of extended π systems. Therefore, six different NHC ligands with a varying number of additional phenyl substituents were used in combination with the monoanionic acetylacetonate (acac) ligand to obtain complexes of the general formula [(NHC)Pt(II)(acac)]. The complexes were fully characterized by standard techniques and advanced spectroscopic methods (¹⁹⁵Pt NMR). For all complexes the solid-state structure determination revealed a square-planar coordination of the platinum atom. Absorption and emission spectra were measured in thin amorphous poly(methyl methacrylate) films at room temperature. Four compounds emit in the blue-green region of the visible spectrum with quantum yields of up to 81%.



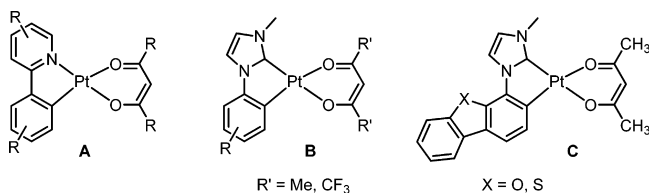
INTRODUCTION

The development of new functional materials has contributed much to the growing demand for energy conservation in everyday life over the past decade.¹ One of the key areas is the modernization of display technologies and domestic lighting,^{2,3} where organometallic chemistry plays an important role. Third-row transition metal complexes have been identified as potential phosphorescent emitters for organic light emitting diodes (OLEDs) with excellent photophysical properties based on the spin–orbit coupling (SOC) induced by the transition-metal atoms,^{4–7} which leads to higher quantum yields. Especially iridium^{8,9} and platinum^{10–15} complexes have attracted much attention in recent years because of their extraordinary photophysical properties.^{16–18} It was found that bi- or tridentate monoanionic ligands, for example, those based on the 2-phenylpyridine fragment, could be cyclometalated to the central metal atom forming ($C^{\wedge}N$) cyclometalated complexes, often with β -diketonate auxiliary ligands (A, Scheme 1).^{12,19,20} In the past years extensive studies of the effect of

modifications of the phenylpyridine ligands on the photophysical properties have been carried out. By extending the π system in the ligand backbone, energy levels can be tuned,^{21,22} and the emission wavelength can be red-shifted as far as the near-infrared region of the spectrum. While the incorporation of aryl systems with low rotational barriers (“soft” dihedrals) bound to the central metal containing fragment often leads to lower quantum yields or ligand-to-ligand charge transfer (LLCT) emission, more rigid systems have shown superior photophysical properties.²³

Complexes of type B (Scheme 1) are a new class of phosphorescent emitters with the carbene carbon atom replacing the nitrogen atom of the $C^{\wedge}N$ cyclometalated complexes (A, Scheme 1).²⁴ It has been shown that by incorporation of a heterocyclic π system (C, Scheme 1) the quantum yields of these complexes increased up to 90%.^{25,26} Therefore, we designed a series of complexes bearing ligands with π systems of different sizes to investigate the influence of those systems and kept acetylacetonate as the auxiliary ligand because of its large highest occupied molecular orbital–lowest unoccupied molecular orbital (HOMO–LUMO) gap to facilitate a *N*-heterocyclic carbene (NHC)-centered, metal-perturbed intraligand charge transfer (ILCT) or rather metal-to-ligand charge transfer (MLCT) emission. The results are compared to the unsubstituted complex of this class of emitters (1, Scheme 1 type B with R = H, R' = Me).²⁵

Scheme 1. General Structure of Cyclometalated Pt(II) Acetylacetonate Complexes



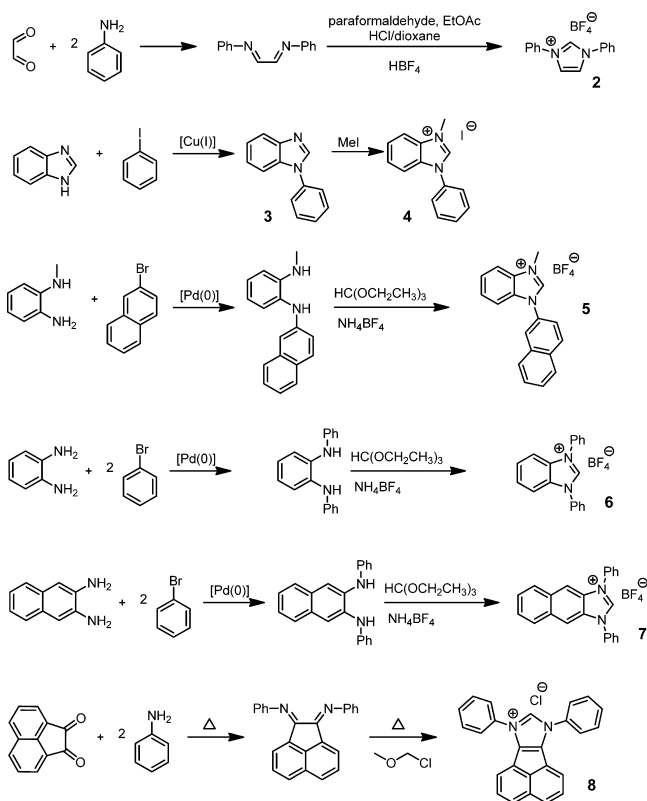
Received: April 25, 2014

Published: May 27, 2014

RESULTS AND DISCUSSION

Design, Synthesis, and Characterization. Ligands with large π systems are known from a number of patents to be of interest for phosphorescent iridium(III) emitters.²⁷ All NHC precursors of this work were designed with specific extensions of the π system in mind regarding the number and position of phenyl rings. To rule out steric or electronic effects from functional groups, only unsubstituted phenyl rings were chosen. Ligand precursor **2** has an additional phenyl ring at the N2 position compared to the 3-methyl-1-phenyl-imidazolium salt that was used for the preparation of the reference complex [(MeImPh)Pt(acac)] **1** (acac = acetylacetonate).²⁵ This phenyl group with a low rotational barrier was incorporated in **6**, **7**, and **8** as well, while these three ligands feature additional extensions of the π system in the heterocyclic backbone. The synthesis of all four compounds starts from a commercially available diamine or α -diketone, which already contains the ligand backbone and thus part of the π extension. Both *N*-substituents in the heterocyclic ring are readily introduced in one reaction step either by condensation with aniline or palladium(0) coupling with an aryl halide (Scheme 2). Both routes would allow for further studies by variation of

Scheme 2. Synthesis of Ligand Precursors 2–8



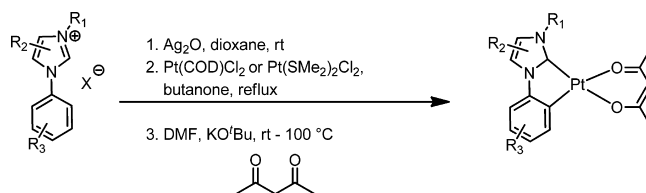
the starting aniline or aryl halide source. The ring closure was accomplished using different reagents. For the synthesis of **2** the intermediate was heated together with paraformaldehyde and HCl, while in the case of **8** the chloromethyl methyl ether was used. Reaction with triethyl orthoformate and ammonium tetrafluoroborate led to compounds **6** and **7**.

For the synthesis of **4** and **5** we used a different approach. The synthesis of **4** involves an Ullmann-type copper(I) catalyzed coupling of benzimidazole and iodobenzene followed by methylation with iodomethane at the N2 position. The

naphthyl substituent in **5** is introduced via a palladium(0) catalyzed coupling of bromonaphthalene and the commercially available *N*-methyl-1,2-phenylenediamine, followed again by ring closure with triethyl orthoformate and ammonium tetrafluoroborate.

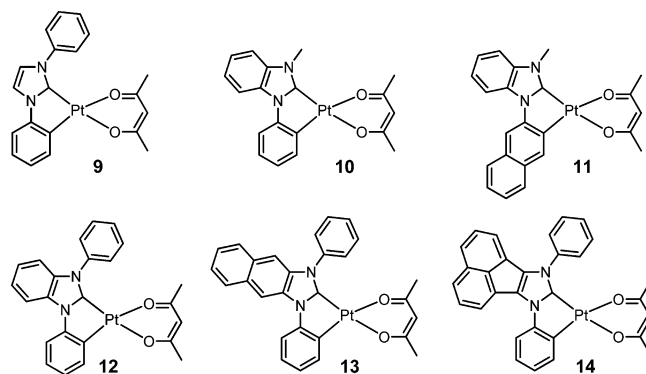
For the synthesis of complexes **9–14** we followed a previously developed route²⁵ (Scheme 3): reaction of the

Scheme 3. Synthesis of Complexes 9–14



imidazolium salt with silver(I) oxide to form the silver(I) NHC complex, transmetalation with dichloro(1,5-cyclooctadiene)-platinum(II) (Pt(COD)Cl₂) without further purification, and treatment with excess acetylacetonate and potassium *tert*-butanolate (KO^tBu) after solvent exchange. The crude product was then washed with water and purified by flash chromatography with methylene chloride on silica gel. The yield of complex **9** turned out to be remarkably high (72%) for such a tedious one-pot reaction. Since the reaction worked quite well with this platinum(II) precursor we used the same route to synthesize the other complexes (Scheme 4). Unfortunately the

Scheme 4. Synthesized Complexes 9–14



yields dropped significantly for the complexes with larger π systems, and while they were still good for **10** (52%) and **12** (53%) and acceptable for **11** (19%) and **14** (11%), complex **13** could only be obtained in traces using dichloro(1,5-cyclooctadiene)-platinum(II). Therefore, we decided to use a different platinum(II) precursor, dichlorobis(dimethyl sulfide)-platinum(II), to obtain **13** in better yields of 18%.

All complexes (Scheme 4) were characterized by standard techniques. The formation of the cyclometalated complexes was verified by the disappearance of the imidazolium protons and the formation of a specific coupling pattern for the cyclometalated rings in the ¹H NMR (see Supporting Information, Figures S1–S6). The ¹⁹⁵Pt NMR spectra for all complexes show chemical shifts from –3335 ppm to –3402 ppm and are characteristic for complexes of this new class of emitters. To assign the different NMR signals a detailed two-dimensional (2D) NMR (COSY, HSQC, HMBC, ROESY) investigation was conducted for complex **11** (see Supporting

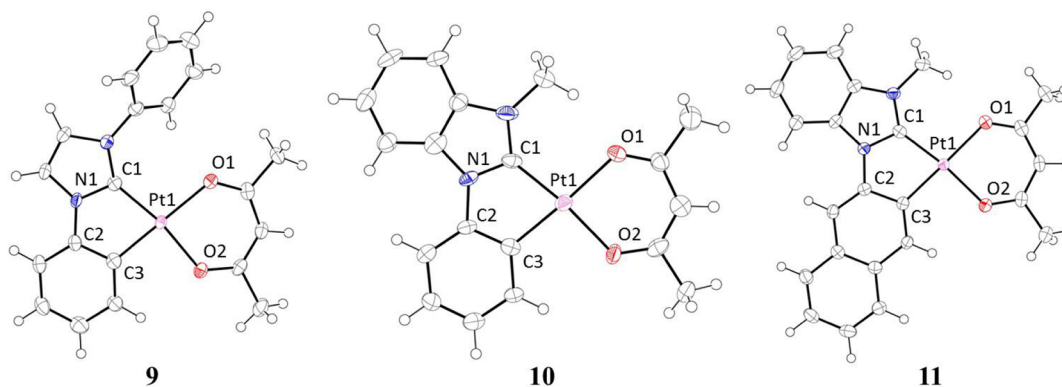


Figure 1. ORTEP^{29,30} representation of 9–11 in the solid state. Thermal ellipsoids are drawn at the 50% probability level.

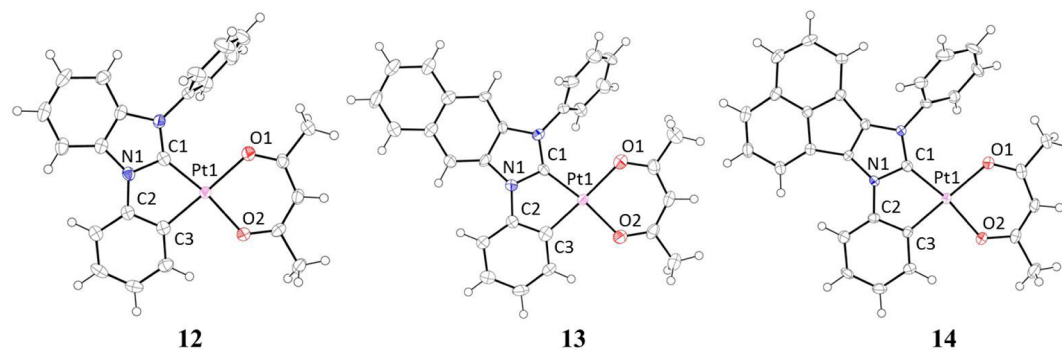


Figure 2. ORTEP^{29,30} representation of 12–14 in the solid state. Thermal ellipsoids are drawn at the 50% probability level.

Table 1. Selected Bond Lengths [Å], Angles, and Dihedral Angles [deg] of Complexes 9–14

bonds [Å], angles [deg]	9	10	11	12	13	14
Pt(1)–C(1)	1.951(5)	1.927(10)	1.927(4)	1.925(3)	1.906(8)	1.955(4)
Pt(1)–C(3)	1.985(5)	2.003(10)	1.973(4)	1.981(2)	1.967(9)	1.975(4)
Pt(1)–O(1)	2.084(4)	2.089(7)	2.094(3)	2.082(2)	2.072(6)	2.086(3)
Pt(1)–O(2)	2.032(3)	2.060(7)	2.047(3)	2.0376(19)	2.034(5)	2.042(3)
O(1)–Pt(1)–O(2)	89.81(4)	89.1(3)	89.42(12)	89.71(8)	90.6(2)	89.38(12)
C(1)–Pt(1)–C(3)	80.1(2)	78.7(4)	80.59(17)	79.87(10)	80.3(3)	80.40(17)
C(2)–N(1)–C(1)–Pt(1)	–0.5(5)	–0.3(11)	0.6(4)	–4.0(3)	–4.5(9)	3.1(5)
N(1)–C(1)–Pt(1)–O(1)	–174.3(3)	–174.1(7)	177.9(3)	–179.30(18)	–170.6(6)	175.2(3)

Information, Figures S7–S10). This compound was chosen to confirm the configuration of the cyclometalated ring because of its good solubility in deuterated dimethyl sulfoxide (DMSO-*d*₆). We prefer to measure in DMSO-*d*₆ over CDCl₃ as we observed partial decomposition of our complexes in CDCl₃, similar to a recently discussed case in the literature.²⁸ The chemical shifts for the carbene carbon atoms, and thus the deshielding, depend strongly on the size of the NHC π system. The signals are observed at 150 ppm for **9**, 161 ppm for **10**, 160 ppm for **11**, 167 ppm for **13**, and 155 ppm for **14** (no signal detected for **12**).

Solid-State Structure Determination. Single crystals suitable for X-ray solid-state determination were obtained for all complexes by slow evaporation of saturated methylene chloride or methylene chloride/acetonitrile solutions. All compounds are 16-valence-electron (16-VE) complexes and exhibit a square-planar geometry around the tetracoordinated platinum(II) center (Figures 1 and 2). For all complexes the phenyl substituents at the N2 position with free dihedral angles are twisted out of the plane of the central metallacycle (C1–N1–C2–C3–Pt1) by 49.0–71.2 degrees. The shortest

platinum-to-ligand contact is the Pt(II) carbene carbon bond (Pt–C1, 1.906–1.955 Å), which is slightly shorter than the Pt–C3 bond to the cyclometalated aryl ring (1.967–2.003 Å). The two Pt–O bonds are just over 2 Å, with the bond opposite of the platinum carbene bond being always a little shorter (Pt1–O1 2.072–2.094 Å, Pt1–O2 2.032–2.060 Å). The differences in the bond lengths around the central metal atom mainly arise from the σ-donating cyclometalated ring and the π-acceptor qualities of the NHC (see Table 1).

Depending on the number of phenyl rings attached to the NHC and especially at the N2 position the complexes exhibit a different packing in the crystal (see Table 2 and Supporting Information, Figures S11–S16). For **9** each complex has two neighboring molecules, one where the acac moieties lie directly above each other (O⋯H contact of 2.59 Å) with a separation of 3.25 Å and a Pt⋯Pt distance of 5.79 Å and another molecule, which is slightly shifted, rotated about 180° and separated by 3.80 Å, while the corresponding Pt⋯Pt distance is only 4.74 Å. The complexes are arranged in two stacks, which themselves form a zigzag pattern throughout the crystal along the *c* axis and meet at an angle of 55° (Supporting Information, Figure S11).

Table 2. Crystal Data and Crystallographic Details for Complexes 9–14

complex	9	10	11	12	13	14
formula	C ₂₀ H ₁₈ N ₂ O ₂ Pt	C ₁₉ H ₁₈ N ₂ O ₂ Pt	C ₂₃ H ₂₀ N ₂ O ₂ Pt	C ₂₄ H ₂₀ N ₂ O ₂ Pt	C ₂₈ H ₂₂ N ₂ O ₂ Pt	C ₃₀ H ₂₂ N ₂ O ₂ Pt
fw [g/mol]	513.46	501.44	551.50	563.50	613.57	637.59
T [K]	198(2)	198(2)	198(2)	198(2)	198(2)	198(2)
wavelength [Å]	0.710 73	0.710 73	0.710 73	0.710 73	0.710 73	0.710 73
crystal system	monoclinic	triclinic	triclinic	monoclinic	monoclinic	triclinic
space group	C2/c	P $\bar{1}$	P $\bar{1}$	P2 ₁ /c	P2 ₁ /c	P $\bar{1}$
a [Å]	21.566(4)	7.6770(15)	7.7870(7)	10.8150(7)	11.274(2)	7.5370(6)
b [Å]	7.8870(16)	10.391(2)	11.3990(5)	15.8080(13)	13.035(3)	9.7140(11)
c [Å]	20.3000(4)	11.254(2)	12.1500(9)	11.7930(14)	18.632(3)	15.372(4)
α [deg]	90	73.86(3)	62.580(4)	90	90	93.589(13)
β [deg]	96.59(3)	78.58(3)	84.406(9)	99.603(7)	126.24(3)	91.396(11)
γ [deg]	90	72.26(3)	78.739(6)	90	90	98.144(7)
U [Å ³]	3430.0(12)	815.0(3)	938.85(12)	1987.9(3)	2208.3(7)	1111.3(3)
Z	8	2	2	4	4	2
D _{calc} [Mg/m ³]	1.989	2.043	1.951	1.883	1.845	1.905
μ (Mo K α) [mm ⁻¹]	8.197	8.622	7.494	7.081	6.383	6.346
crystal size [mm ³]	0.50 × 0.39 × 0.22	0.34 × 0.27 × 0.25	0.53 × 0.27 × 0.17	0.26 × 0.35 × 0.53	0.58 × 0.41 × 0.37	0.57 × 0.35 × 0.18
F(000)	1968	480	532	1088	1192	620
refl. collected	39 889	13 929	19 731	45 152	46 959	27 548
independent refl.	3511 [R _{int} = 0.042]	2978 [R _{int} = 0.118]	3825 [R _{int} = 0.033]	4059 [R _{int} = 0.027]	4448 [R _{int} = 0.079]	4574 [R _{int} = 0.047]
GOF on F ²	1.251	1.094	1.300	1.210	1.199	1.166
R ₁ [I > 2 σ (I)]	0.0208	0.0532	0.0164	0.0142	0.0326	0.0249
wR ₂	0.0598	0.1209	0.0569	0.0339	0.0954	0.0552
data/restr/param	3511/0/228	2978/0/220	3825/0/256	4059/0/264	4448/0/300	4574/0/318

The structure of complex **10** is relatively planar, as the methyl group at the N2 atom allows for an ordered structure that forms only one stack along the *a* axis, wherein the complexes form pairs (Supporting Information, Figure S12). These are separated by 3.38 Å with a Pt...Pt distance of 3.30 Å, which is slightly below the sum of the van der Waals radii, indicating a weak metal–metal interaction. The distance to the next platinum atom in the stack is 4.94 Å. Within the pairs, the NHC moiety of one complex is oriented toward the acac ligand of the second molecule. The solid-state structure of **11** also forms a layered packing of two complexes, each in a distance of just 3.37 Å with a Pt...Pt contact of 5.45 Å (Supporting Information, Figure S13). They interact with the surrounding molecules via their respective acac auxiliary ligands, which are aligned on top of each other with an O...H contact of 2.67 Å.

Complexes **12** and **13** crystallize in a similar way as **9**, with two stacks again forming a zigzag pattern and a superstructure of the two complexes oriented toward each other with a long Pt...Pt distance of 6.20/5.04 Å (plane-to-plane 3.42/3.74 Å, Supporting Information, Figures S14 and S15). Compound **14** has a similar molecular structure as **12** and **13** but forms layers along the *c* axis (Supporting Information, Figure S16). Each molecule has two different neighboring complexes in the next layer. To one of them the respective NHC moieties are aligned above each other, while for the other complex the acac ligands interact (O...H contact 2.68 Å).

In summary the more planar complexes **10** and **11** with only methyl groups at the N2 position are more densely packed and show the shortest Pt...Pt contacts. The bond lengths and angles around the central platinum atom found for these new complexes are in good agreement with the few previously published structures of this type.^{15,25,26,31–35}

Photophysical Studies. The ultraviolet–visible (UV–vis) absorption and emission spectra of all complexes were studied

at room temperature (rt). To investigate intermolecular interactions arising from the different π systems during the photoluminescence process, efforts were made to create pure amorphous emitter films (100%) from solution. Unfortunately early crystallization was observed for **13** and **14**, therefore no emission data could be obtained. Absorption spectra of the amorphous (**9**–**12**) and crystallized (**13**, **14**) pure films show a different number of peaks between 220 and 355 nm (Supporting Information, Figure S17). The intense high-energy transitions (<250 nm) might be ascribed to spin-allowed NHC-centered $^1\pi-\pi^*$ transitions followed by mixed MLCT transitions. While complexes **9**–**13** show similar spectra, the spectrum of complex **14** is quite different since it does not display a defined fine structure and shows only two bands (236 and 328 nm).

Furthermore, the absorption spectra were also measured in thin poly(methyl methacrylate) (PMMA) films doped with 2 wt % emitter (Figure 3). The individual spectra are all very similar compared to the measurements in pure films.

Because of the premature crystallization of **13** and **14** emission spectra for pure films could only be measured of **9**–**12** (Supporting Information, Figure S18). While **9**, **10**, and **12** each show a single broad emission band in the green region, indicating excimer formation or even direct Pt–Pt interaction, the spectrum of **11** is typical for an ILCT emission showing vibronic coupling. To investigate these effects in more detail concentration-dependent measurements in PMMA films were done for complex **10** (see Supporting Information, Figure S19). For the different concentrations a change in the shape of the curves was observed. The higher concentrations show a more prominent emission toward 550 nm, similar to the emission in the 100% film. The quantum yields obtained were remarkably high for the pure emitter films: 3% (**9**), 14.2% (**10**, $\tau_0 = 2.9 \mu\text{s}$),

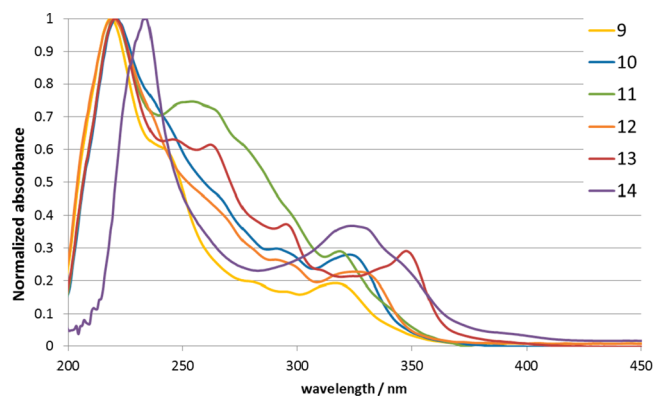


Figure 3. Absorption spectra of complexes 9–14 (2 wt % in PMMA at rt).

21.7% (**11**, $\tau_0 = 66.4 \mu\text{s}$), and 31% (**12**, $\tau_0 = 9.2 \mu\text{s}$) ($\tau_0 =$ decay lifetime).

The emission spectra of complexes 9–13 in 2 wt % PMMA films (Figure 4) exhibit at least three distinct emission maxima.

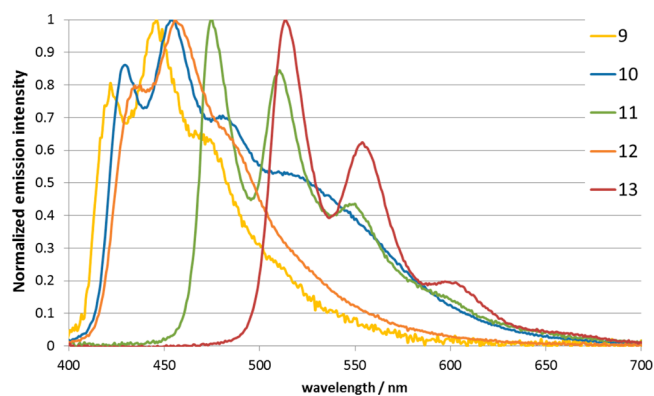


Figure 4. Emission spectra of complexes 9–13 (2 wt % in PMMA at rt).

The quantum yield of complex **14** was below the detection limit of the quantum yield measurement system (ca. 1–2%). For the complexes **9** (Commission Internationale de l'Éclairage (CIE) 0.155; 0.110) and **10** (0.197; 0.238) with the smallest π extension, the first emission peak lies in the deep blue region, with the emission maximum at around 450 nm and additional shoulders reaching into the green region of the spectrum. With even larger π systems the emission is subsequently red-shifted with the exception of **12**, which remains a true blue emitter (CIE 0.158; 0.147). The emission maximum for complex **11** (CIE 0.235; 0.458) with two additional phenyl rings compared to the reference complex **1** (CIE 0.190; 0.190) is considerably red-shifted to 476 nm, with weaker peaks at 508 and 550 nm.

With the addition of another phenyl ring to the NHC the emission becomes even more red-shifted for complex **13** (CIE 0.323; 0.628) with emissions at 515, 554, and 600 nm. The color changes with increasing size of the π system to higher wavelengths can be explained by the resulting stabilization of the LUMO and thus a smaller energy gap between the singlet ground state and the first excited emissive state. As can be seen in the emission profiles, all complexes show vibronic coupling, which is in good agreement with an NHC ligand-centered ILCT process. The distance between the individual peaks is in the range of 1200 to 1430 cm^{-1} and corresponds to NHC-centered vibrations as determined by density functional theory (DFT) calculations.

In Table 3 the photophysical results for the measurements in PMMA are given. It is interesting to note that the highest quantum yield was found for complex **13** with the largest π system accessible for measurement. Even the incorporation of only one phenyl ring at the N2 position of the NHC increases the quantum yield from 7%²⁵ for **1** to nearly 17% for **9**. As expected, the addition of a phenyl ring in the NHC backbone instead of the N2 position has a greater effect due to a higher contribution of π electrons to the frontier molecular orbitals (FMOs) increasing the quantum yield to 40% (**10**). Further extension can again increase the quantum efficiency but has a strong impact on the emission color. Complexes **11** and **13** (with the larger π system) were found to have significantly longer decay lifetimes (**11**, 183 μs ; **13**, 405 μs). The values for **9**, **10**, and **12** are similar to those measured before for this class of emitters.²⁵

Electrochemistry. For all complexes cyclic voltammetry and differential pulse voltammetry experiments were conducted in anhydrous dimethylformamide (DMF) under inert conditions with 0.1 M *n*-Bu₄NPF₆ (TBAPF₆) as supporting electrolyte to improve the conductivity. All presented potentials derived from differential pulse voltammetry are relative to the ferrocene/ferrocenium (Fc/Fc⁺) redox couple used as an internal reference. Ionization potentials (IP) and electron affinities (EA) were calculated according to a relationship developed by Forrest and co-workers.^{36,37} Complex **9**, with only one additional phenyl ring attached at the N2 position in comparison to a reference complex **1** (Scheme 1, R = H, R' = Me),²⁵ was found to have the most cathodic reduction potential and thus the least electron affinity (EA = 1.31 eV, quasireversible), while complexes **10–12**, with a π extension in the imidazole backbone, showed EAs of 1.44 eV (**10**, reversible), 1.47 eV (**11**, irreversible), and 1.45 eV (**12**, irreversible). Since the reduction is considered to involve the LUMO, which is according to DFT calculations mainly localized on the NHC ligand, the lower EA values of **10–12** can be attributed to the expanded π system of the cyclometalated NHC ligands, which can more easily accommodate

Table 3. Photoluminescence Data (2 wt % in PMMA, rt) of the Cyclometalated Complexes 9–13

	λ_{exc} [nm] ^a	CIE x _r ;y _r ^b	λ_{em} [nm] ^c	ϕ^d	τ_0 [μs] ^e	k_r [10^3 s^{-1}] ^f	k_{nr} [10^3 s^{-1}] ^g
9	355	0.155;0.110	446	0.17	18.3	54.8	275.2
10	330	0.197;0.238	454	0.40	8.0	124.4	189.0
11	355	0.235;0.458	476	0.58	183.0	5.5	3.9
12	340	0.158;0.147	457	0.41	9.2	108.4	154.7
13	370	0.323;0.628	515	0.81	404.6	2.5	0.6

^aExcitation wavelength. ^bCIE coordinates at rt. ^cMaximum emission wavelength. ^dQuantum yield at λ_{exc} , N₂ atmosphere. ^eDecay lifetimes (excited by laser pulses (355 nm, 1 ns)) given as $\tau_0 = \tau_v/\phi$. ^f $k_r = \phi/\tau_0$. ^g $k_{\text{nr}} = (1 - \phi)/\tau_0$.

the negative charge. In this regard, the highest EAs were found for the complexes with the greatest π extension, namely, **13** (1.76 eV, reversible) and **14** (2.46 eV, first cycle reversible; second cycle irreversible). These observations are in line with related Pt(II) systems that bear C[^]N cyclometalated ligands.^{12,21,38} All compounds undergo an irreversible oxidation with ionization potentials of 5.59 (**9**), 5.68 (**10**), 5.41 (**11**), 5.72 (**12**), 5.64 (**13**), and 5.40 eV (**14**). DFT calculations show a participation of platinum d orbitals in the HOMO, which is otherwise delocalized over the NHC ligand. Thus, a metal oxidation (Pt(II) \rightarrow Pt(III)) is possible, and the irreversibility of the oxidation could be explained by nucleophilic attack of solvents at the square-planar Pt(III) center, which usually defines the redox properties of Pt(II).¹² Although the irreversibility of the electrochemical processes might be a problem when using the data to estimate the HOMO–LUMO separation, a decreasing gap is found with an expansion of the π system at the NHC ligand as is consistent with the expectations. The cyclic voltammograms are given in the Supporting Information, Figures S20–S25.

Computational Studies. Geometry optimizations for the singlet and triplet states were performed using DFT methods (B3LYP/6-31G(d)). To gain further insight into the photophysical properties of the complexes, frontier molecular orbitals (FMOs) (Supporting Information, Figure S26) and spin densities (Supporting Information, Figure S27) were computed for the optimized structures (based on Kohn–Sham orbitals) to better understand the photophysical process and derive the participation of the ligands and the platinum atom in the emission process. The HOMO for each complex is mainly composed of the cyclometalated aryl group and platinum d orbitals, with some differing contributions from the imidazole fragment and the acac ligand. When comparing the HOMOs of the complexes it becomes obvious that the phenyl substituents at the N2 atom seem to be taking no part. This is quite feasible since the HOMO is of π orbital character and the phenyl substituents are twisted out of the complex plane. We found that with an increasing size of the π system the contribution from the acac ligand to the FMOs becomes less notable.

With the changes in the ligand backbone (mainly an extension of the π system) the calculated HOMO–LUMO gap decreases significantly. The calculated S_0 – S_1 gap follows the order **9** (4.67 eV) > **10** (4.27 eV) > **12** (4.23 eV) > **11** (4.05 eV) > **13** (3.72 eV) and **14** (3.03 eV). This is in excellent agreement with the experimentally observed emission maxima, which are 446 nm (**9**), 454 nm (**10**), 457 nm (**12**), 476 nm (**11**), and 515 nm (**13**). The energy gaps between the S_0 and T_1 states (both at their optimized geometries) were found to be 2.49 eV (**9**), 2.80 eV (**10**), 2.54 eV (**11**), 2.78 eV (**12**), 2.02 eV (**13**), and 1.61 eV (**14**). With the exception of the value for complex **9**, these follow the same order as above.

The DFT-optimized geometries are also in good agreement with the data from the solid-state structure determination (see Supporting Information, Tables S1–S6). Upon excitation to the triplet state most complexes retain their geometry with the exception of **9** and **12**, which bend significantly out of planarity (see Supporting Information, Figure S28).

The quite different photophysical properties of these six complexes depend on the number of phenyl groups and the size of the π system. With an increasing number of phenyl rings the quantum yield generally increases, and the emission maximum is red-shifted in agreement with a smaller HOMO–LUMO gap of the complexes. Comparing the

influence of a phenyl ring at the N2 atom or at the backbone of the ligand we found that the former is less pronounced. The rigidity of the system plays an important role for the observed quantum yields, as geometry changes between the singlet and triplet state seem to reduce it (see Photophysical Studies).²³

CONCLUSION

We present the synthesis and characterization of six new C[^]C* cyclometalated platinum(II) NHC complexes and their ligands. The solid-state structure determination revealed a square-planar coordination of the central platinum atom for all complexes. Five of the complexes were found to be phosphorescent emitters with an emission in the blue to green region of the visible spectrum, characteristic band structures, and good to very good quantum yields of up to 81%. The number of phenyl groups attached to the NHC ligand and their position exhibit a significant effect on the photophysical properties. Quantum-chemical DFT calculations are in good agreement with the experimentally observed properties. Our results demonstrate that changing the size of the π system and the right choice of aryl substituents allows the tuning of the photophysical properties of this class of novel C[^]C* cyclometalated platinum(II) emitters.

EXPERIMENTAL SECTION

General Comments. Solvents of 99.5% purity were used throughout this study. 1,4-Dioxane and DMF were dried using standard techniques and stored under an argon atmosphere over molecular sieves (4 Å). Dichloro(1,5-cyclooctadiene)platinum(II)³⁹ was prepared following a modified literature procedure.²⁵ Dichlorobis-(dimethyl sulfide)platinum(II) was prepared according to a literature procedure.⁴⁰ Potassium tetrachloroplatinate(II) was obtained from Pressure Chemicals Co. All other chemicals were obtained from common suppliers and used without further purification. ¹H, ¹³C, and ¹⁹⁵Pt NMR spectra were recorded on a Bruker NMR spectrometer (300 MHz, 500 MHz, 600 MHz). ¹H and ¹³C NMR spectra were referenced internally using the resonances of the solvent (¹H: 7.26, ¹³C: 77.0 for CDCl₃; ¹H: 2.50, ¹³C: 39.43 for DMSO-*d*₆). ¹⁹F NMR spectra were referenced externally against trifluoromethylbenzene (F₃C–C₆H₅). ¹⁹⁵Pt NMR spectra were referenced externally using potassium tetrachloroplatinate(II) in D₂O (–1617.2 (PtCl₄²⁻), –2654.1 (PtCl₂)). Shifts are given in ppm, and coupling constants *J* are given in Hz. Elemental analyses were performed by the microanalytical laboratory of our institute on a Hekatech elemental analyzer. Melting points have been determined using a Wagner and Munz Poly Therm A system and are not corrected.

Photoluminescence. The photoluminescence of the complexes was measured in thin PMMA films doped with 2 wt % emitter and in 100% emitter films. The 2 wt % films were prepared by doctor blading a solution of emitter (2 mg/mL) in a 10 wt % PMMA solution in dichloromethane on a substrate with a 60 μ m doctor blade. The film was dried, and the emission was measured under nitrogen. The excitation was carried out at a wavelength of 330–370 nm (Xe lamp with monochromator), and the emission was detected with a calibrated quantum-yield detections system (Hamamatsu, model C9920–02). The phosphorescence decay was measured by excitation with pulses of a third harmonic generation Nd:YAG laser (355 nm, 1 ns) and time-resolved photon counting in the multichannel scaling (MCS) technique.

Electrochemistry. Cyclic voltammetry and differential pulsed voltammetry were performed using a computer-controlled Metrohm Autolab PGSTAT12 potentiostat in a three-electrode single-compartment cell with a platinum working electrode, a platinum wire counter electrode, and a Ag/AgCl reference electrode. Anhydrous DMF (distilled over P₂O₅) was used as the solvent under an inert atmosphere, and 0.1 M TBAPF₆ was used as the supporting electrolyte. The measurements were conducted with 1 mM solutions

of the corresponding complex at rt with a scan rate of 0.1 V/s. All potentials were internally referenced to the ferrocene/ferrocenium (Fc/Fc⁺) couple. The IP (HOMO) and EA (LUMO) levels were calculated using the following equations: (1) IP [eV] = 1.4*(1.0x $E_{\text{onset}}^{\text{Fc/Fc}^+}$ - Fc/Fc⁺ $E_{\text{onset}}^{\text{Fc/Fc}^+}$) + 4.6³⁶ and (2) EA [eV] = 1.19*(1.Red $E_{1/2}^{\text{Fc/Fc}^+}$ - Fc/Fc⁺ $E_{1/2}^{\text{Fc/Fc}^+}$) + 4.78.³⁷

Synthesis. 1,3-Diphenyl-1H-imidazolium tetrafluoroborate (2). The ligand precursor **2** was synthesized by modifying a known literature procedure.⁴¹ Aniline (4.66 g, 50 mmol) was dissolved in 80 mL of methanol, and 40 wt % aqueous glyoxal solution (2.82 mL, 25 mmol) was added before the mixture was stirred for 72 h at rt. The mixture was evaporated to dryness, and the residue was dissolved in 70 mL of ethyl acetate. Paraformaldehyde (0.94 g, 31.3 mmol) was added before 4 M hydrochloric acid in 1,4-dioxane (9.4 mL, 37.5 mmol) was slowly added. After it was stirred for 3 h, the reaction was quenched by addition of a saturated sodium bicarbonate solution. The aqueous phase was extracted twice with 100 mL of diethyl ether before 50 wt % fluoroboric acid (5.5 mL) was slowly added to the aqueous phase. The precipitated solid was collected, washed with water, and dried *in vacuo*. Yield: 0.77 g, 10%. ¹H NMR (DMSO-*d*₆, 300.13 MHz): δ 10.34 (s, 1H, NCHN), 8.58 (d, *J* = 1.4 Hz, 2H, NCH), 7.92 (d, *J* = 7.6 Hz, 4H, CCH_{arom}), 7.72 (t, *J* = 7.6 Hz, 4H, CH_{arom}), 7.64 (t, *J* = 7.6 Hz, 2H, CH_{arom}) ppm. ¹³C NMR (DMSO-*d*₆, 75.475 MHz): δ 134.6 (C_i), 134.5 (NCHN), 130.1 (CH_{arom}), 130.0 (CH_{arom}), 122.0 (CH_{arom}), 121.9 (CH_{arom}) ppm. ¹⁹F NMR (DMSO-*d*₆, 282.4 MHz): δ -148.9 ppm. Melting poing (mp) 132–134 °C. Anal. Calcd for C₁₅H₁₃BF₄N₂ (308.1 g mol⁻¹): C, 58.48; H, 4.25; N, 9.09. Found: C, 58.23; H, 4.01; N, 8.92%.

1-Phenyl-1H-benzo[d]imidazole (3). A literature procedure⁴² was modified in a way that benzimidazole (1.77 g, 15.0 mmol), iodobenzene (2.04 g, 10.0 mmol), potassium hydroxide (1.12 g, 20.0 mmol), and copper(I) oxide (0.22 g, 1.5 mmol) were suspended in 25 mL of dry DMSO and stirred under argon for 24 h at 120 °C. After it was cooled, the reaction mixture was poured into 30 mL of water and extracted with 3 × 50 mL of ethyl acetate. The combined organic layers were washed with 50 mL of brine and dried over MgSO₄. The crude product was purified by flash chromatography using silica gel with ethyl acetate as eluent. Yield: 1.31 g, 67%. Analytical data are in agreement with the literature. ¹H NMR (CDCl₃, 300.13 MHz): δ 8.14 (s, 1H, NCHN), 7.89 (m, 1H, CH_{arom}), 7.52 (m, 6H, CH_{arom}), 7.35 (m, 2H, CH_{arom}) ppm.

3-Methyl-1-phenyl-1H-benzo[d]imidazolium iodide (4). A known literature procedure⁴³ was modified in a way that compound **3** (388 mg, 2.0 mmol) and iodomethane (426 mg, 3.0 mmol) were dissolved in 3 mL of tetrahydrofuran (THF) in a pressure tube and heated to 100 °C. The reaction was stirred for 24 h, and the resulting solid was filtered off, washed with THF and diethyl ether, and dried *in vacuo*. Yield: 616 mg, 92%. Analytical data are in agreement with the literature. ¹H NMR (DMSO-*d*₆, 300.13 MHz): δ 10.12 (s, 1H, NCHN), 8.16 (d, *J* = 8.0 Hz, 1H, CH_{arom}), 7.77 (m, 8H, CH_{arom}), 4.17 (s, 3H, CH₃) ppm. ¹³C NMR (DMSO-*d*₆, 75.475 MHz): δ 143.0 (NCHN), 133.1 (C_i), 131.8 (C_i), 130.8 (C_i), 130.3 (CH_{arom}), 127.3 (CH_{arom}), 126.8 (CH_{arom}), 125.0 (CH_{arom}), 113.8 (CH_{arom}), 113.2 (CH_{arom}), 33.4 (CH₃) ppm.

3-Methyl-1-(naphthalene-2-yl)-1H-benzo[d]imidazolium tetrafluoroborate (5). In an argon-flushed Schlenk tube 2-bromonaphthalene (42.80 g, 206.7 mmol) and *N*-methyl-1,2-phenylenediamine (25.00 g, 204.6 mmol) were dissolved in 500 mL of dry toluene. Tris(dibenzylideneacetone)dipalladium(0) (Pd₂(dba)₃, 1.88 g, 2.1 mmol), 9,9-dimethyl-4,5-bis(diphenylphosphino)xanthene (xantphos, 3.56 g, 6.1 mmol), and sodium *tert*-butanolate (27.70 g, 285.4 mmol) were added, and the resulting mixture was heated to reflux for 15 h. After it was cooled to rt, water was added to the reaction mixture, which was extracted, and the combined organic phases were washed with water, dried over sodium sulfate, filtered, and evaporated to dryness. Flash chromatography with cyclohexane, toluene, and ethyl acetate gave the corresponding intermediate. Part of the intermediate (3.10 g, 12.5 mmol) was suspended in triethyl orthoformate (26.00 g, 174.8 mmol) under inert conditions before addition of ammonium tetrafluoroborate (1.30 g, 12.5 mmol). The mixture was heated to

reflux for 6 h, cooled to rt, and the yellow precipitate was filtered off, washed with petroleum ether, triethyl orthoformate, and 3 mL of dichloromethane (DCM). The crude product was further purified by dissolving the dried solid in DCM, filtration, and removal of all volatile compounds. Yield: 2.55 g, 59%. ¹H NMR (DMSO-*d*₆, 500.13 MHz): δ 10.23 (s, 1H, NCHN), 8.45 (d, *J* = 2.1 Hz, 1H, CH_{arom}), 8.33 (d, *J* = 8.7 Hz, 1H, CH_{arom}), 8.19 (d, *J* = 8.3 Hz, 1H, CH_{arom}), 8.16 (m, 2H, CH_{arom}), 7.96 (d, *J* = 8.3 Hz, 1H, CH_{arom}), 7.91 (dd, *J* = 2.1 Hz, *J* = 8.3 Hz, 1H, CH_{arom}), 7.82 (t, *J* = 7.7 Hz, 1H, CH_{arom}), 7.76 (d, *J* = 7.5 Hz, 1H, CH_{arom}), 7.74 (m, 2H, CH_{arom}), 4.22 (s, 3H, CH₃) ppm. ¹³C NMR (DMSO-*d*₆, 125.75 MHz): δ 143.3 (NCHN), 133.0 (C_i), 132.7 (C_i), 131.9 (C_i), 130.9 (C_i), 130.6 (C_i), 130.5 (CH_{arom}), 128.3 (CH_{arom}), 128.0 (CH_{arom}), 127.9 (CH_{arom}), 127.8 (CH_{arom}), 127.4 (CH_{arom}), 126.9 (CH_{arom}), 124.0 (CH_{arom}), 122.2 (CH_{arom}), 113.9 (CH_{arom}), 113.5 (CH_{arom}), 33.4 (CH₃) ppm. ¹⁹F NMR (DMSO-*d*₆, 282.4 MHz): δ -148.89 ppm. mp 160–161 °C. Anal. Calcd for C₁₈H₁₅BF₄N₂ (346.1 g mol⁻¹): C, 62.46; H, 4.37; N, 8.09. Found: C, 62.25; H, 4.14; N, 8.05%.

1,3-Diphenyl-1H-benzo[d]imidazolium tetrafluoroborate (6). To a mixture of 1,2-phenylenediamine (97.30 g, 882.0 mmol) and distilled bromobenzene (283.10 g, 1785.0 mmol) in degassed toluene, Pd₂(dba)₃ (8.00 g, 8.7 mmol), xantphos (15.30 g, 25.6 mmol), distilled water (23.2 mL, 1287.0 mmol), and sodium *tert*-butanolate (170.00 g, 1764.0 mmol) were added, and the resulting mixture was heated to reflux for 5 h. After it was cooled to rt, the precipitate was filtered off and washed with toluene. Flash chromatography with toluene gave the corresponding intermediate. Part of the intermediate (140.0 g, 537.8 mmol) was suspended in 1.62 L of triethyl orthoformate under inert conditions before addition of ammonium tetrafluoroborate (58.10 g, 537.8 mmol). The mixture was heated to reflux for 18 h and then cooled to rt, and the precipitate was filtered off and washed with petroleum ether and triethyl orthoformate. The crude product was further purified by dissolving the dried solid in DCM, filtration, and removal of all volatile compounds. Yield: 174.88 g, 91%. ¹H NMR (DMSO-*d*₆, 300.13 MHz): δ 10.57 (s, 1H, NCHN), 7.95 (m, 6H, CH_{arom}), 7.79 (m, 8H, CH_{arom}) ppm. ¹³C NMR (DMSO-*d*₆, 75.475 MHz): δ 142.7 (NCHN), 132.9 (C_i), 131.1 (C_i), 130.6 (CH_{arom}), 130.4 (CH_{arom}), 127.7 (CH_{arom}), 125.3 (CH_{arom}), 113.7 (CH_{arom}) ppm. ¹⁹F NMR (DMSO-*d*₆, 282.4 MHz): δ -148.92 ppm.

1,3-Diphenyl-1H-naphtho[2,3-d]imidazolium tetrafluoroborate (7). In an argon-flushed Schlenk tube, 2,3-diaminonaphthalene (26.5 g, 167.5 mmol) and distilled bromobenzene (57.85 g, 368.5 mmol) were dissolved in 500 mL of dry toluene. Pd₂(dba)₃ (1.53 g, 1.7 mmol), xantphos (2.91 g, 5.0 mmol), and sodium *tert*-butanolate (32.20 g, 335.0 mmol) were added to the solution. The mixture was then heated to reflux for 12 h. After cooling to rt, water was added to the reaction mixture, which was extracted, and the combined organic phases were washed with water, dried over sodium sulfate, filtered, and evaporated to dryness. Flash chromatography with DCM gave the corresponding intermediate. The intermediate (43.30 g, 139.5 mmol) was suspended in triethyl orthoformate (290.00 g, 1950.0 mmol) under inert conditions before addition of ammonium tetrafluoroborate (14.60 g, 24.7 mmol). The mixture was heated to reflux for 8 h and then cooled to rt, and the precipitate was filtered off and washed with petroleum ether and triethyl orthoformate. The crude product was further purified by dissolving the dried solid in DCM, filtration, and removal of all volatile compounds. Yield: 42.75 g, 75%. ¹H NMR (DMSO-*d*₆, 500.13 MHz): δ 10.75 (s, 1H, NCHN), 8.61 (s, 2H, CH_{arom}), 8.30 (dd, *J* = 3.3 Hz, *J* = 6.4 Hz, 2H, CH_{arom}), 8.05 (d, *J* = 7.8 Hz, 4H, CH_{arom}), 7.87 (t, *J* = 7.8 Hz, 4H, CH_{arom}), 7.80 (t, *J* = 7.6 Hz, 2H, CH_{arom}), 7.69 (dd, *J* = 3.3 Hz, *J* = 6.4 Hz, 2H, CH_{arom}) ppm. ¹³C NMR (DMSO-*d*₆, 125.75 MHz): δ 146.5 (NCHN), 133.1 (C_i), 131.4 (C_i), 130.6 (CH_{arom}), 130.4 (CH_{arom}), 130.2 (C_i), 128.4 (CH_{arom}), 126.9 (CH_{arom}), 125.4 (CH_{arom}), 111.2 (CH_{arom}) ppm. ¹⁹F NMR (DMSO-*d*₆, 282.4 MHz): δ -148.92 ppm. mp 256–258 °C. Anal. Calcd for C₂₃H₁₇BF₄N₂ (408.2 g mol⁻¹): C, 67.67; H, 4.20; N, 6.86. Found: C, 67.33; H, 4.16; N, 6.78%.

7,9-Diphenyl-7H-acenaphtho[1,2-d]imidazolium chloride - BIAN (8). The ligand precursor **8** was prepared according to a literature procedure⁴⁴ in two steps. In a 10 mL glacial acetic acid solution

acenaphthenequinone (0.91 g, 5.0 mmol), aniline (1.16 g, 12.5 mmol, 1.14 mL), and zinc chloride (1.36 g, 10.0 mmol) were heated to reflux and stirred for 1 h. After it was cooled to rt, the reaction mixture was filtered and washed with acetic acid and diethyl ether. The dried solid was suspended in 12 mL of water and heated to reflux with 12 g of potassium carbonate for 2 h under intense stirring. The red solid was collected by filtration, washed with water, and dried *in vacuo*. Then 0.33 g (1.0 mmol) of the obtained solid was heated to 100 °C in chloromethyl methyl ether (2.01 g, 25.0 mmol, 1.90 mL) in a pressure tube for 16 h. After it was cooled to rt the product was precipitated with diethyl ether, filtered, washed with diethyl ether, and dried *in vacuo*. Yield: 0.37 g, 96%. Analytical data are in agreement with the literature. ¹H NMR (DMSO-*d*₆, 300.13 MHz): δ 10.21 (s, 1H, NCHN), 8.23 (d, *J* = 8.1 Hz, 2H, CH_{arom}), 8.13 (d, *J* = 7.5 Hz, 4H, CH_{arom}), 7.92–7.76 (m, 10H, CH_{arom}) ppm.

(SP-4-3)-[1,3-Diphenyl-1H-imidazol-2-ylidene-κC2,κC2']-(2,4-pentanedionato-κO2,κO4) platinum(II) (9). A dried and argon-flushed Schlenk tube was charged with compound 2 (246 mg, 0.8 mmol) and silver(I) oxide (94 mg, 0.4 mmol). After addition of 20 mL of dry 1,4-dioxane the reaction mixture was stirred under argon in the dark at rt for 21 h. Pt(COD)Cl₂ (299 mg, 0.8 mmol) and 10 mL of 2-butanone were added, and the mixture was heated to 115 °C and stirred for another 21 h. Afterward, all volatiles were removed under reduced pressure, and KO^tBu (366 mg, 3.2 mmol), acetylacetone (0.33 mL, 3.2 mmol), and 20 mL of dry DMF were added under argon. After this was stirred for 20 h at rt and 6 h at 100 °C, all volatiles were again removed under reduced pressure, leaving the crude product, which was washed with water and purified by flash chromatography with methylene chloride (silica gel KG60). After drying *in vacuo* a pale yellow solid was obtained. Yield: 296 mg, 72%. ¹H NMR (CDCl₃, 300.13 MHz): δ 7.81 (dd, *pseudo*-triplet, *J*₁ = 1.9 Hz, *J*₂ = 7.0 Hz, *J*_{H,Pt} = 26.4 Hz, 1H, PtCCH_{arom}), 7.59 (m, 2H, CH_{arom}), 7.45 (m, 3H, CH_{arom}), 7.38 (d, *J* = 2.1 Hz, 1H, NCCCH_{arom}), 7.03 (m, 4H, CH_{arom}), 5.3 (s, 1H, CH), 1.98 (s, 3H, CH₃), 1.36 (s, 3H, CH₃) ppm. ¹³C NMR (CDCl₃, 75.475 MHz): δ 184.9 (CO), 184.0 (CO), 150.4 (NCN), 146.6 (CPt), 138.4 (C_i), 131.7 (CH_{arom}), 128.7 (CH_{arom}), 128.5 (CH_{arom}), 126.8 (CH_{arom}), 125.5 (C_i), 124.4 (CH_{arom}), 123.4 (CH_{arom}), 121.3 (CH_{arom}), 114.5 (CH_{arom}), 110.2 (CH_{arom}), 101.6 (CH), 27.6 (CH₃), 27.1 (CH₃) ppm. ¹⁹⁵Pt NMR (CDCl₃, 64.52 MHz): δ -3402 ppm. mp 197–199 °C. Anal. Calcd for C₂₀H₁₈N₂O₂Pt (513.5 g mol⁻¹): C, 46.78; H, 3.53; N, 5.46. Found: C, 46.91; H, 3.31; N, 5.36%.

(SP-4-3)-[3-Methyl-1-phenyl-1H-benzo[d]imidazol-2-ylidene-κC2,κC2']-(2,4-pentanedionato-κO2,κO4)platinum(II) (10). A dried and argon-flushed Schlenk tube was charged with compound 4 (269 mg, 0.8 mmol) and silver(I) oxide (94 mg, 0.4 mmol). After addition of 20 mL of dry 1,4-dioxane the reaction mixture was stirred under argon in the dark at rt for 21 h. Pt(COD)Cl₂ (299 mg, 0.8 mmol) and 10 mL of 2-butanone were added, and the mixture was heated to 115 °C and stirred for another 21 h. Afterward, all volatiles were removed under reduced pressure, and KO^tBu (366 mg, 3.2 mmol), acetylacetone (0.33 mL, 3.2 mmol), and 20 mL of dry DMF were added under argon. After this was stirred for 20 h at rt and for 6 h at 100 °C, all volatiles were again removed under reduced pressure, leaving the crude product, which was washed with water and purified by flash chromatography with methylene chloride (silica gel KG60). After drying *in vacuo* a yellow solid was obtained. Yield: 209 mg, 52%. ¹H NMR (CDCl₃, 300.13 MHz): δ 7.89 (m, 2H, PtCH_{arom}, CH_{arom}), 7.47 (d, *J* = 7.8 Hz, 1H, CH_{arom}), 7.35 (m, 3H, CH_{arom}), 7.13 (dt, *J*₁ = 1.3 Hz, *J*₂ = 7.6 Hz, 1H, CH_{arom}), 7.03 (dt, *J*₁ = 1.0 Hz, *J*₂ = 7.4 Hz, 1H, CH_{arom}), 5.52 (s, 1H, CH), 4.26 (s, 3H, NCH₃), 2.08 (s, 3H, CH₃), 2.01 (s, 3H, CH₃) ppm. ¹³C NMR (CDCl₃, 75.475 MHz): δ 185.2 (CO), 160.7 (NCN), 148.1 (CPt), 135.5 (C_i), 131.3 (C_i), 131.2 (CH_{arom}), 125.3 (C_i), 124.1 (CH_{arom}), 123.7 (CH_{arom}), 123.4 (CH_{arom}), 122.7 (CH_{arom}), 111.3 (CH_{arom}), 110.8 (CH_{arom}), 110.4 (CH_{arom}), 102.0 (CH), 31.2 (NCH₃), 28.0 (CH₃), 27.9 (CH₃) ppm. ¹⁹⁵Pt NMR (CDCl₃, 64.52 MHz): δ -3395 ppm. mp 177–179 °C. Anal. Calcd for C₁₉H₁₈N₂O₂Pt (501.4 g mol⁻¹): C, 45.51; H, 3.62; N, 5.59. Found: C, 45.48; H, 3.74; N, 5.62%.

(SP-4-3)-[3-Methyl-1-(naphthalene-3-yl)-1H-benzo[d]imidazol-2-ylidene-κC2,κC2']-(2,4-pentanedionato-κO2,κO4)platinum(II) (11). A dried and argon-flushed Schlenk tube was charged with compound 5 (277 mg, 0.8 mmol) and silver(I) oxide (94 mg, 0.4 mmol). After addition of 20 mL of dry 1,4-dioxane the reaction mixture was stirred under argon in the dark at rt for 21 h. Pt(COD)Cl₂ (299 mg, 0.8 mmol) and 10 mL of 2-butanone were added, and the mixture was heated to 115 °C and stirred for another 21 h. Afterward, all volatiles were removed under reduced pressure, and KO^tBu (366 mg, 3.2 mmol), acetylacetone (0.33 mL, 3.2 mmol), and 20 mL of dry DMF were added under argon. After this was stirred for 20 h at rt and for 6 h at 100 °C, all volatiles were again removed under reduced pressure, leaving the crude product, which was washed with water and purified by flash chromatography with methylene chloride (silica gel KG60). After drying *in vacuo* a yellow-green solid was obtained. Yield: 85 mg, 19%. ¹H NMR (DMSO-*d*₆, 600.16 MHz): δ 8.52 (d, *J* = 8.1 Hz, 1H, CH_{arom}), 8.22 (s, 1H, CH_{arom}), 8.06 (s, 1H, CH_{arom}), 7.98 (d, *J* = 7.6 Hz, 1H, CH_{arom}), 7.76 (m, 2H, CH_{arom}), 7.54 (dt, *J*₁ = 1.1 Hz, *J*₂ = 8.0 Hz, 1H, CH_{arom}), 7.50 (t, *J* = 7.3 Hz, 1H, CH_{arom}), 7.38 (m, 2H, CH_{arom}), 5.67 (s, 1H, CH), 4.29 (s, 3H, NCH₃), 2.12 (s, 3H, CH₃), 2.02 (s, 3H, CH₃) ppm. ¹³C NMR (DMSO-*d*₆, 150.91 MHz): δ 185.3 (CO), 184.9 (CO), 159.6 (NCN), 146.4 (CPt), 135.4 (C_i), 131.6 (C_i), 130.3 (C_i), 130.0 (C_i), 128.6 (CH_{arom}), 127.7 (CH_{arom}), 126.3 (CH_{arom}), 124.8 (CH_{arom}), 124.6 (CH_{arom}), 124.4 (C_i), 124.2 (CH_{arom}), 123.6 (CH_{arom}), 111.6 (CH_{arom}), 111.5 (CH_{arom}), 108.1 (CH_{arom}), 101.9 (CH), 31.2 (NCH₃), 27.7 (CH₃), 27.6 (CH₃) ppm. ¹⁹⁵Pt NMR (DMSO-*d*₆, 128.56 MHz): δ -3335 ppm. mp 245–246 °C. Anal. Calcd for C₂₃H₂₀N₂O₂Pt (551.5 g mol⁻¹): C, 50.09; H, 3.66; N, 5.08. Found: C, 50.33; H, 3.72; N, 5.09%.

(SP-4-3)-[1,3-Diphenyl-1H-benzo[d]imidazol-2-ylidene-κC2,κC2']-(2,4-pentanedionato-κO2,κO4)platinum(II) (12). A dried and argon-flushed Schlenk tube was charged with compound 6 (287 mg, 0.8 mmol) and silver(I) oxide (94 mg, 0.4 mmol). After addition of 20 mL of dry 1,4-dioxane the reaction mixture was stirred under argon in the dark at rt for 21 h. Pt(COD)Cl₂ (299 mg, 0.8 mmol) and 10 mL of 2-butanone were added, and the mixture was heated to 115 °C and stirred for another 21 h. Afterward, all volatiles were removed under reduced pressure, and KO^tBu (366 mg, 3.2 mmol), acetylacetone (0.33 mL, 3.2 mmol), and 20 mL of dry DMF were added under argon. After this was stirred for 20 h at rt and for 6 h at 100 °C, all volatiles were again removed under reduced pressure, leaving the crude product, which was washed with water and purified by flash chromatography with methylene chloride (silica gel KG60). After drying *in vacuo* a light yellow solid was obtained. Yield: 241 mg, 53%. ¹H NMR (CDCl₃, 300.13 MHz): δ 8.04 (d, *J* = 8.2 Hz, 1H, CH_{arom}), 7.92 (dd, *pseudo*-triplet, *J*₁ = 1.4 Hz, *J*₂ = 7.4 Hz, *J*_{H,Pt} = 27.0 Hz, 1H, PtCCH_{arom}), 7.57 (m, 6H, CH_{arom}), 7.41 (t, *J* = 7.8 Hz, 1H, CH_{arom}), 7.27 (t, *J* = 7.8 Hz, 1H, CH_{arom}), 7.19 (dt, *J*₁ = 1.4 Hz, *J*₂ = 7.6 Hz, 1H, CH_{arom}), 7.12 (d, *J* = 7.4 Hz, 1H, CH_{arom}), 7.09 (dt, *J*₁ = 1.4 Hz, *J*₂ = 7.6 Hz, 1H, CH_{arom}), 5.31 (s, 1H, CH), 2.01 (s, 3H, CH₃), 1.31 (s, 3H, CH₃) ppm. ¹³C NMR (CDCl₃, 75.475 MHz): δ 185.4 (CO), 184.1 (CO), 148.0 (CPt), 136.5 (C_i), 136.2 (C_i), 131.5 (CH_{arom}), 131.0 (C_i), 129.2 (CH_{arom}), 129.1 (CH_{arom}), 128.4 (CH_{arom}), 126.2 (C_i), 124.5 (CH_{arom}), 123.8 (CH_{arom}), 123.7 (CH_{arom}), 123.1 (CH_{arom}), 111.8 (CH_{arom}), 111.5 (CH_{arom}), 110.9 (CH_{arom}), 101.7 (CH), 27.6 (CH₃), 27.1 (CH₃) ppm. ¹⁹⁵Pt NMR (CDCl₃, 64.52 MHz): δ -3379 ppm. mp 231–233 °C. Anal. Calcd for C₂₄H₂₀N₂O₂Pt (563.5 g mol⁻¹): C, 51.15; H, 3.58; N, 4.97. Found: C, 51.38; H, 3.63; N, 4.87%.

(SP-4-3)-[1,3-Diphenyl-1H-naphtho[2,3-*d*]imidazol-2-ylidene-κC2,κC2']-(2,4-pentanedionato-κO2,κO4)platinum(II) (13). A dried and argon-flushed Schlenk tube was charged with 1,3-diphenyl-1H-naphtho[2,3-*d*]imidazolium tetrafluoroborate 7 (327 mg, 0.8 mmol) and silver(I) oxide (94 mg, 0.4 mmol). After addition of 20 mL of dry 1,4-dioxane the reaction mixture was stirred under argon in the dark at rt for 21 h. Dichlorobis(dimethyl sulfide)platinum(II) (312 mg, 0.8 mmol) and 10 mL of 2-butanone were added, and the mixture was heated to 115 °C and stirred for another 21 h. Afterward, all volatiles were removed under reduced pressure, and KO^tBu (366 mg, 3.2 mmol), acetylacetone (0.33 mL, 3.2 mmol), and 20 mL of dry DMF were added under argon. After this was stirred for 20 h at rt and for 6 h

at 100 °C, all volatiles were again removed under reduced pressure, leaving the crude product, which was washed with water and purified by flash chromatography with methylene chloride (silica gel KG60). After drying *in vacuo* a yellow solid was obtained. Yield: 89 mg, 18%. ¹H NMR (CDCl₃, 300.13 MHz): δ 8.41 (s, 1H, CH_{arom}), 8.06 (d, *J* = 8.0 Hz, 1H, CH_{arom}), 7.96 (dd, *J*₁ = 1.0 Hz, *J*₂ = 7.4 Hz, 1H, CH_{arom}), 7.82 (d, *J* = 8.4 Hz, 1H, CH_{arom}), 7.75 (d, *J* = 7.8 Hz, 1H, CH_{arom}), 7.67 (m, 2H, CH_{arom}), 7.62 (m, 3H, CH_{arom}), 7.50 (m, 3H, CH_{arom}), 7.26 (t, 1H, CH_{arom}), 7.12 (t, *J* = 7.3 Hz, 1H, CH_{arom}), 5.33 (s, 1H, CH), 2.02 (s, 3H, CH₃), 1.33 (s, 3H, CH₃) ppm. ¹³C NMR (CDCl₃, 75.475 MHz): δ 185.5 (CO), 184.2 (CO), 166.8 (NCN), 147.9 (Cpt), 136.7 (C_i), 136.4 (C_i), 131.4 (CH_{arom}), 131.0 (C_i), 130.5 (C_i), 129.7 (C_i), 129.3 (CH_{arom}), 129.2 (CH_{arom}), 128.6 (CH_{arom}), 128.1 (CH_{arom}), 127.9 (CH_{arom}), 126.0 (C_i), 125.8 (CH_{arom}), 125.3 (CH_{arom}), 123.9 (CH_{arom}), 123.7 (CH_{arom}), 111.8 (CH_{arom}), 108.0 (CH_{arom}), 107.3 (CH_{arom}), 101.7 (CH), 27.5 (CH₃), 27.1 (CH₃) ppm. ¹⁹⁵Pt NMR (CDCl₃, 64.52 MHz): δ -3336 ppm. mp 285–289 °C. Anal. Calcd for C₂₈H₂₂N₂O₂Pt (613.6 g mol⁻¹): C, 54.81; H, 3.61; N, 4.57. Found: C, 54.70; H, 3.56; N, 4.62%.

(*SP-4-3*)-[7,9-Diphenyl-7H-acenaphtho[1,2-d]imidazol-2-ylidene-κC₈,κC'₂']-[2,4-pentanedionato-κO₂,κO₄]platinum(II) (**14**). A dried and argon-flushed Schlenk tube was charged with compound **8** (305 mg, 0.8 mmol) and silver(I) oxide (94 mg, 0.4 mmol). After addition of 20 mL of dry 1,4-dioxane the reaction mixture was stirred under argon in the dark at rt for 21 h. Pt(COD)Cl₂ (299 mg, 0.8 mmol) and 10 mL of 2-butanone were added, and the mixture was heated to 115 °C and stirred for another 21 h. Afterward, all volatiles were removed under reduced pressure, and KO^tBu (366 mg, 3.2 mmol), acetylacetone (0.33 mL, 3.2 mmol), and 20 mL of dry DMF were added under argon. After this was stirred for 20 h at rt and for 6 h at 100 °C, all volatiles were again removed under reduced pressure, leaving the crude product, which was washed with water and purified by flash chromatography with methylene chloride (silica gel KG60). After drying *in vacuo* a red crystalline solid was obtained. Yield: 55 mg, 11%. ¹H NMR (CDCl₃, 300.13 MHz): δ 8.19 (d, *J* = 7.2 Hz, 1H, CH_{arom}), 7.92 (dd, *J*₁ = 1.4 Hz, *J*₂ = 7.5 Hz, 1H, CH_{arom}), 7.81 (m, 4H, CH_{arom}), 7.67 (m, 2H, CH_{arom}), 7.59 (m, 3H, CH_{arom}), 7.40 (dd, *J*₁ = 7.0 Hz, *J*₂ = 8.2 Hz, 1H, CH_{arom}), 7.22 (dd, *J*₁ = 1.4 Hz, *J*₂ = 7.5 Hz, 1H, CH_{arom}), 7.14 (d, *J* = 6.7 Hz, 1H, CH_{arom}), 7.09 (dd, *J*₁ = 1.4 Hz, *J*₂ = 7.5 Hz, 1H, CH_{arom}), 5.31 (s, 1H, CH), 2.00 (s, 3H, CH₃), 1.34 (s, 3H, CH₃) ppm. ¹³C NMR (CDCl₃, 150.91 MHz): δ 185.0 (CO), 184.0 (CO), 155.3 (NCN), 146.9 (Cpt), 137.4 (C_i), 131.8 (CH_{arom}), 130.0 (C_i), 129.6 (C_i), 129.4 (CH_{arom}), 129.1 (CH_{arom}), 128.2 (CH_{arom}), 127.7 (CH_{arom}), 127.6 (CH_{arom}), 127.4 (CH_{arom}), 127.3 (CH_{arom}), 126.0 (C_i), 125.8 (C_i), 125.7 (C_i), 124.3 (CH_{arom}), 123.7 (CH_{arom}), 123.6 (CH_{arom}), 120.5 (CH_{arom}), 111.8 (CH_{arom}), 101.7 (CH), 27.6 (CH₃), 27.1 (CH₃) ppm. ¹⁹⁵Pt NMR (CDCl₃, 64.52 MHz): δ -3376 ppm. mp 312–315 °C. Anal. Calcd for C₃₀H₂₂N₂O₂Pt (637.6 g mol⁻¹): C, 56.51; H, 3.48; N, 4.39. Found: C, 56.12; H, 3.36; N, 4.39%.

X-ray Crystallography. Preliminary examination and data collection were carried out on an area detecting system (Kappa-CCD; Nonius, FR590) using graphite monochromated Mo K α radiation (λ = 0.710 73 Å) with an Oxford Cryosystems cooling system at the window of a sealed fine-focus X-ray tube. The reflections were integrated. Raw data were corrected for Lorentz, polarization, decay, and absorption effects. The absorption correction was applied using SADABS.⁴⁵ After merging, the independent reflections were used for all calculations. The structure was solved by a combination of direct methods⁴⁶ and difference Fourier syntheses.⁴⁷ All non-hydrogen atom positions were refined with anisotropic displacement parameters. Hydrogen atoms were placed in ideal positions using the SHELXL riding model. Full-matrix least-squares refinements were carried out by minimizing $\sum w(F_o^2 - F_c^2)^2$ with the SHELXL-97 weighting scheme and stopped at shift/err < 0.001. Details of the structure determinations are given in the Supporting Information. Neutral-atom scattering factors for all atoms and anomalous dispersion corrections for the non-hydrogen atoms were taken from International Tables for Crystallography.⁴⁸ All calculations were performed with the programs COLLECT,⁴⁹ DIRAX,⁵⁰ EVALCCD,⁵¹ SIR92,⁴⁶ SADABS,⁴⁵

PLATON,⁵² and the SHELXL-97 package.^{47,53} For the visualization, Mercury⁵⁴ and ORTEP-III^{29,30} were used, and for the preparation of the Supporting Information, ENCIFER⁵⁵ and the WinGX⁵⁶ suite were used.

Computational Details. All calculations were performed with the Gaussian09 package.⁵⁷ The density functional hybrid model B3LYP^{58–62} was used together with the 6-31G(d)^{63–68} basis set. No symmetry or internal coordinate constraints were applied during optimizations. All reported intermediates were verified as true minima by the absence of negative eigenvalues in the vibrational frequency analysis. Harmonic force constants were calculated for all geometries to verify them as ground states. In all cases platinum was described using a decontracted Hay–Wadt (*n* + 1) effective core potential and basis set.^{69–71} HOMO and LUMO FMOs were computed on the singlet ground-state structure, while the spin densities were calculated based on the ground-state structure of the optimized triplet state. Approximate free energies were obtained through thermochemical analysis, using the thermal correction to Gibbs free energy as reported by Gaussian09. This takes into account zero-point effects, thermal enthalpy corrections, and entropy. All energies reported in this paper, unless otherwise noted, are free energies at standard conditions (*T* = 298 K, *p* = 1 atm), using unscaled frequencies. For visualization, GaussView⁷² and CYLview⁷³ were used.

■ ASSOCIATED CONTENT

📄 Supporting Information

The crystallographic data for compounds **9–14** in CIF format, packing diagrams for compounds **9–14**, 2D NMR spectra, cyclic and differential pulse voltammograms, FMOs and spin densities as well as Cartesian coordinates for the optimized structures. This material is available free of charge via the Internet at <http://pubs.acs.org>

■ AUTHOR INFORMATION

✉ Corresponding Author

*E-mail: thomas.strassner@chemie.tu-dresden.de. Fax: 49 351 46339679. Phone: 49 351 46338571.

📍 Present Address

[§](A.P.) Anorganische Chemie, TU München, Lichtenbergstrasse 4, 85747 Garching, Germany.

📝 Notes

The authors declare no competing financial interest.

■ ACKNOWLEDGMENTS

We are very grateful to I. Stengel (BASF) for the measurement of the cyclic and differential pulse voltammograms, and to Dr. Fuchs (BASF) and Dr. Lennartz (BASF) for helpful discussions. We also thank the ZIH for computation time on their high-performance computing facility and the BMBF (FKZ: 13N10477) for funding.

■ REFERENCES

- (1) Crabtree, R. H. *Organometallics* **2011**, *30*, 17–19.
- (2) Forrest, S. R. *Nature* **2004**, *428*, 911–918.
- (3) Reineke, S.; Lindner, F.; Schwartz, G.; Seidler, N.; Walzer, K.; Luessem, B.; Leo, K. *Nature* **2009**, *459*, 234–238.
- (4) Baldo, M. A.; O'Brien, D. F.; You, Y.; Shoustikov, A.; Sibley, S.; Thompson, M. E.; Forrest, S. R. *Nature* **1998**, *395*, 151–154.
- (5) Kwong, R. C.; Lamansky, S.; Thompson, M. E. *Adv. Mater.* **2000**, *12*, 1134–1138.
- (6) *Highly Efficient OLEDs with Phosphorescent Materials*; Yersin, H., Ed.; Wiley-VCH Verlag GmbH & Co. KGaA: Weinheim, Germany, 2008; pp 438.
- (7) Sasabe, H.; Kido, J. *Chem. Mater.* **2011**, *23*, 621–630.

- (8) Lamansky, S.; Djurovich, P.; Murphy, D.; Abdel-Razzaq, F.; Lee, H.-E.; Adachi, C.; Burrows, P. E.; Forrest, S. R.; Thompson, M. E. *J. Am. Chem. Soc.* **2001**, *123*, 4304–4312.
- (9) Tsuboyama, A.; Okada, S.; Ueno, K. In *Highly Efficient Red-Phosphorescent Iridium Complexes*; Wiley-VCH: Weinheim, Germany, 2008; pp 163–183.
- (10) Hissler, M.; Connick, W. B.; Geiger, D. K.; McGarrah, J. E.; Lipa, D.; Lachicotte, R. J.; Eisenberg, R. *Inorg. Chem.* **2000**, *39*, 447–457.
- (11) Chan, S.-C.; Chan, M. C. W.; Wang, Y.; Che, C.-M.; Cheung, K.-K.; Zhu, N. *Chem.—Eur. J.* **2001**, *7*, 4180–4190.
- (12) Brooks, J.; Babayan, Y.; Lamansky, S.; Djurovich, P. I.; Tsyba, I.; Bau, R.; Thompson, M. E. *Inorg. Chem.* **2002**, *41*, 3055–3066.
- (13) Pomestchenko, I. E.; Luman, C. R.; Hissler, M.; Ziesse, R.; Castellano, F. N. *Inorg. Chem.* **2003**, *42*, 1394–1396.
- (14) Kalinowski, J.; Fattori, V.; Cocchi, M.; Williams, J. A. G. *Coord. Chem. Rev.* **2011**, *255*, 2401–2425.
- (15) Hudson, Z. M.; Sun, C.; Helander, M. G.; Chang, Y.-L.; Lu, Z.-H.; Wang, S. *J. Am. Chem. Soc.* **2012**, *134*, 13930–13933.
- (16) Chou, P.-T.; Chi, Y. *Chem.—Eur. J.* **2007**, *13*, 380–395.
- (17) Murphy, L.; Williams, J. A. G. *Top. Organomet. Chem.* **2010**, *28*, 75–111.
- (18) Rausch, A. F.; Homeier, H. H. H.; Yersin, H. *Top. Organomet. Chem.* **2010**, *29*, 193–235.
- (19) D'Andrade, B. W.; Brooks, J.; Adamovich, V.; Thompson, M. E.; Forrest, S. R. *Adv. Mater.* **2002**, *14*, 1032–1036.
- (20) Wong, W.-Y.; He, Z.; So, S.-K.; Tong, K.-L.; Lin, Z. *Organometallics* **2005**, *24*, 4079–4082.
- (21) Bossi, A.; Rausch, A. F.; Leitl, M. J.; Czerwieńiec, R.; Whited, M. T.; Djurovich, P. I.; Yersin, H.; Thompson, M. E. *Inorg. Chem.* **2013**, *52*, 12403–12415.
- (22) Xu, X.; Zhao, Y.; Dang, J.; Yang, X.; Zhou, G.; Ma, D.; Wang, L.; Wong, W.-Y.; Wu, Z.; Zhao, X. *Eur. J. Inorg. Chem.* **2012**, *2012*, 2278–2288.
- (23) Rausch, A. F.; Murphy, L.; Williams, J. A. G.; Yersin, H. *Inorg. Chem.* **2012**, *51*, 312–319.
- (24) Egen, M.; Kahle, K.; Bold, M.; Gessner, T.; Lennartz, C.; Nord, S.; Schmidt, H.-W.; Thelakkat, M.; Baete, M.; Neuber, C.; Kowalsky, W.; Schildknecht, C.; Johannes, H.-H. Preparation of Transition Metal N-heterocyclic Carbene Complexes for Use in Organic Light-Emitting Diodes (OLEDs). WO2006056418A2, 2006.
- (25) Unger, Y.; Meyer, D.; Molt, O.; Schildknecht, C.; Muenster, I.; Wagenblast, G.; Strassner, T. *Angew. Chem., Int. Ed.* **2010**, *49*, 10214–10216.
- (26) Tronnier, A.; Risler, A.; Langer, N.; Wagenblast, G.; Muenster, I.; Strassner, T. *Organometallics* **2012**, *31*, 7447–7452.
- (27) Thompson, M. E.; Tamayo, A.; Djurovich, P.; Sajoto, T.; Forrest, S. R.; Mackenzie, P. B.; Walters, R.; Brooks, J.; Li, X.-C.; Alleyne, B.; Tsai, J.-Y.; Lin, C.; Ma, B.; Barone, M. S.; Kwong, R. Organic Light-Emitting Devices Employing Organometallic Compounds, Especially Luminescent Compounds with Carbene Ligands, and Selected Compounds. WO2005113704A2, 2005.
- (28) Baranoff, E.; Curchod, B. F. E.; Frey, J.; Scopelliti, R.; Kessler, F.; Tavernelli, I.; Rothlisberger, U.; Gratzel, M.; Nazeeruddin, M. K. *Inorg. Chem.* **2012**, *51*, 215–224.
- (29) Farrugia, L. J. *J. Appl. Crystallogr.* **1997**, *30*, 565.
- (30) Burnett, M. N.; Johnson, C. K. *ORTEP-III*; Oak Ridge National Laboratory: Oak Ridge, TN, 1996.
- (31) Tenne, M.; Unger, Y.; Strassner, T. *Acta Crystallogr., Sect. C: Cryst. Struct. Commun.* **2012**, *68*, m203–m205.
- (32) Tronnier, A.; Nischan, N.; Strassner, T. *J. Organomet. Chem.* **2013**, *730*, 37–43.
- (33) Tronnier, A.; Nischan, N.; Metz, S.; Wagenblast, G.; Muenster, I.; Strassner, T. *Eur. J. Inorg. Chem.* **2014**, *2014*, 256–264.
- (34) Tronnier, A.; Metz, S.; Wagenblast, G.; Muenster, I.; Strassner, T. *Dalton Trans.* **2014**, *43*, 3297–3305.
- (35) Tronnier, A.; Poethig, A.; Herdtweck, E.; Strassner, T. *Organometallics* **2014**, *33*, 898–908.
- (36) D'Andrade, B. W.; Datta, S.; Forrest, S. R.; Djurovich, P.; Polikarpov, E.; Thompson, M. E. *Org. Electron.* **2005**, *6*, 11–20.
- (37) Djurovich, P. I.; Mayo, E. I.; Forrest, S. R.; Thompson, M. E. *Org. Electron.* **2009**, *10*, 515–520.
- (38) Ghedini, M.; Pugliese, T.; La Deda, M.; Godbert, N.; Aiello, I.; Amati, M.; Belviso, S.; Lelj, F.; Accorsi, G.; Barigelletti, F. *Dalton Trans.* **2008**, 4303–4318.
- (39) Drew, D.; Doyle, J. R. *Inorg. Synth.* **1990**, *28*, 346–349.
- (40) Otto, S.; Roodt, A. *J. Organomet. Chem.* **2006**, *691*, 4626–4632.
- (41) Clavier, H.; Correa, A.; Cavallo, L.; Escudero-Adan, E. C.; Benet-Buchholz, J.; Slawin, A. M. Z.; Nolan, S. P. *Eur. J. Inorg. Chem.* **2009**, 1767–1773.
- (42) Huang, Y.-Z.; Miao, H.; Zhang, Q.-H.; Chen, C.; Xu, J. *Catal. Lett.* **2008**, *122*, 344–348.
- (43) Tennyson, A. G.; Rosen, E. L.; Collins, M. S.; Lynch, V. M.; Bielawski, C. W. *Inorg. Chem.* **2009**, *48*, 6924–6933.
- (44) Vasudevan, K. V.; Butorac, R. R.; Abernethy, C. D.; Cowley, A. H. *Dalton Trans.* **2010**, *39*, 7401–7408.
- (45) Sheldrick, G. M. *SADABS*, Version 2.10; University of Goettingen: Goettingen, Germany, 2002.
- (46) Altomare, A.; Cascarano, G.; Giacovazzo, C.; Guagliardi, A.; Burla, M. C.; Polidori, G.; Camalli, M. *J. Appl. Crystallogr.* **1994**, *27*, 435.
- (47) Sheldrick, G. M. *Acta Crystallogr., Sect. A: Found. Crystallogr.* **2008**, *A64*, 112–122.
- (48) *International Tables for Crystallography, Vol. C: Mathematical, Physical and Chemical Tables*; Wilson, A. J. C., Ed.; Kluwer (Springer-Verlag): New York, 1992; pp 900.
- (49) Hooft, R. W. W. *Data Collection Software for Nonius-Kappa CCD*; Nonius B.V.: Delft, The Netherlands, 1999.
- (50) Duisenberg, A. J. M. *J. Appl. Crystallogr.* **1992**, *25*, 92–96.
- (51) Duisenberg, A. J. M.; Kroon-Batenburg, L. M. J.; Schreurs, A. M. M. *J. Appl. Crystallogr.* **2003**, *36*, 220–229.
- (52) Spek, A. L. *Acta Crystallogr.* **2009**, *D65*, 148–155.
- (53) Sheldrick, G. M. *SHELXL-97, Program for the Refinement of Structures*; University of Goettingen: Goettingen, Germany, 1997.
- (54) Macrae, C. F.; Bruno, I. J.; Chisholm, J. A.; Edgington, P. R.; McCabe, P.; Pidcock, E.; Rodriguez-Monge, L.; Taylor, R.; van, d. S. J.; Wood, P. A. *J. Appl. Crystallogr.* **2008**, *41*, 466–470.
- (55) Allen, F. H.; Johnson, O.; Shields, G. P.; Smith, B. R.; Towler, M. *J. Appl. Crystallogr.* **2004**, *37*, 335–338.
- (56) Farrugia, L. J. *J. Appl. Crystallogr.* **1999**, *32*, 837–838.
- (57) Frisch, M. J.; Trucks, G. W.; Schlegel, H. B.; Scuseria, G. E.; Robb, M. A.; Cheeseman, J. R.; Scalmani, G.; Barone, V.; Mennucci, B.; Petersson, G. A.; Nakatsuji, H.; Caricato, M.; Li, X.; Hratchian, H. P.; Izmaylov, A. F.; Bloino, J.; Zheng, G.; Sonnenberg, J. L.; Hada, M.; Ehara, M.; Toyota, K.; Fukuda, R.; Hasegawa, J.; Ishida, M.; Nakajima, T.; Honda, Y.; Kitao, O.; Nakai, H.; Vreven, T.; Montgomery, Jr., J. A.; Peralta, J. E.; Ogliaro, F.; Bearpark, M.; Heyd, J. J.; Brothers, E.; Kudin, K. N.; Staroverov, V. N.; Kobayashi, R.; Normand, J.; Raghavachari, K.; Rendell, A.; Burant, J. C.; Iyengar, S. S.; Tomasi, J.; Cossi, M.; Rega, N.; Millam, J. M.; Klene, M.; Knox, J. E.; Cross, J. B.; Bakken, V.; Adamo, C.; Jaramillo, J.; Gomperts, R.; Stratmann, R. E.; Yazyev, O.; Austin, A. J.; Cammi, R.; Pomelli, C.; Ochterski, J. W.; Martin, R. L.; Morokuma, K.; Zakrzewski, V. G.; Voth, G. A.; Salvador, P.; Dannenberg, J. J.; Dapprich, S.; Daniels, A. D.; Farkas, Ö.; Foresman, J. B.; Ortiz, J. V.; Cioslowski, J.; Fox, D. J. *Gaussian 09, Revision B.01*; Gaussian, Inc.: Wallingford, CT, 2009.
- (58) Vosko, S. H.; Wilk, L.; Nusair, M. *Can. J. Phys.* **1980**, *58*, 1200–1211.
- (59) Becke, A. D. *Phys. Rev. A: At., Mol., Opt. Phys.* **1988**, *38*, 3098–3100.
- (60) Lee, C.; Yang, W.; Parr, R. G. *Phys. Rev. B: Condens. Matter Mater. Phys.* **1988**, *37*, 785–789.
- (61) Miehlich, B.; Savin, A.; Stoll, H.; Preuss, H. *Chem. Phys. Lett.* **1989**, *157*, 200–206.
- (62) Stephens, P. J.; Devlin, F. J.; Chabalowski, C. F.; Frisch, M. J. *J. Phys. Chem.* **1994**, *98*, 11623–11627.

- (63) Ditchfield, R.; Hehre, W. J.; Pople, J. A. *J. Chem. Phys.* **1971**, *54*, 724–728.
- (64) Hehre, W. J.; Ditchfield, R.; Pople, J. A. *J. Chem. Phys.* **1972**, *56*, 2257–2261.
- (65) Hariharan, P. C.; Pople, J. A. *Chem. Phys. Lett.* **1972**, *16*, 217–219.
- (66) Hariharan, P. C.; Pople, J. A. *Theor. Chim. Acta* **1973**, *28*, 213–222.
- (67) Hariharan, P. C.; Pople, J. A. *Mol. Phys.* **1974**, *27*, 209–214.
- (68) Rassolov, V. A.; Pople, J. A.; Ratner, M. A.; Windus, T. L. *J. Chem. Phys.* **1998**, *109*, 1223–1229.
- (69) Hay, P. J.; Wadt, W. R. *J. Chem. Phys.* **1985**, *82*, 270–283.
- (70) Hay, P. J.; Wadt, W. R. *J. Chem. Phys.* **1985**, *82*, 299–310.
- (71) Wadt, W. R.; Hay, P. J. *J. Chem. Phys.* **1985**, *82*, 284–298.
- (72) Dennington, R. L.; Keith, T.; Millam, J. M.; Eppinnett, W.; Hovell, W. L.; Gilliland, R. *GaussView*, 3.09; Gaussian Inc.: Wallingford, CT, 2003.
- (73) Legault, C. Y. *CYLVview*, 1.0b; Université de Sherbrooke: Sherbrooke, Canada, 2009.